ISSN 1063-780X, Plasma Physics Reports, 2016, Vol. 42, No. 3, pp. 269–277. © Pleiades Publishing, Ltd., 2016.
Original Russian Text © S.S. Ananyev, S.A. Dan'ko, V.V. Myalton, A.I. Zhuzhunashvili, Yu.G. Kalinin, V.I. Krauz, M.S. Ladygina, A.K. Marchenko, 2016, published in Fizika Plazmy, 2016, Vol. 42, No. 3, pp. 282–290.

PLASMA DYNAMICS

Spectroscopic Measurements of the Parameters of the Helium Plasma Jets Generated in the Plasma Focus Discharge at the PF-3 Facility

S. S. Ananyev[a], S. A. Dan'ko[a], V. V. Myalton[a], A. I. Zhuzhunashvili[a], Yu. G. Kalinin[a], V. I. Krauz[a], M. S. Ladygina[b], and A. K. Marchenko[b]

[a] *National Research Centre Kurchatov Institute, pl. Akademika Kurchatova 1, Moscow, 123182 Russia*
[b] *National Science Center Kharkiv Institute of Physics and Technology, Akademichna vul. 1, Kharkiv, 61108 Ukraine*
e-mail: Danko_SA@nrcki.ru, Ananev_SS@nrcki.ru

Received May 21, 2015; in final form, October 22, 2015

Abstract—The spectroscopic technique used to measure the parameters of the plasma jets generated in the plasma focus discharge and those of the plasma of the immobile gas through which these jets propagate is described. The time evolution of the intensities and shapes of spectral lines in experiments carried out with helium at the PF-3 facility was studied by means of electron-optical streak cameras. The plasma electron temperature, $T \approx 4$–5 eV, was determined from the intensity ratio of two spectral lines, one of which ($\lambda_1 = 5876$ Å) belongs to neutral helium, while the other ($\lambda_2 = 4686$ Å), to hydrogen-like helium ions. The plasma density at different time instants was determined from the Stark broadening of these lines in the electric fields of different nature. The plasma density is found to vary from 4×10^{14} to 2×10^{17} cm^{-3}.

DOI: 10.1134/S1063780X16030028

1. INTRODUCTION

At present, experiments on the generation of intense plasma flows are being carried out at the PF-3 facility (National Research Centre Kurchatov Institute). Studies of the dynamics of such flows and the determination of their parameters can be useful in constructing a model of astrophysical jets propagating to giant distances [1]. Analysis shows that laboratory plasma jets can be efficiently used to model nonrelativistic jets observed in young stars [2]. In connection with this, the necessity arises to determine the density and temperature of both the plasma jet itself and the background plasma in which the jet propagates. In this paper, the spectroscopic technique used to determine the density and temperature of plasma in experiments on the generation and transportation of helium plasma jets at the PF-3 facility is described and results obtained by means of this technique are presented.

The main goal of the experiments was to adjust the technique for measuring the parameters of weakly ionized plasma formed in the drift chamber as a result of the action of an ionizing radiation pulse from the plasma focus (PF) on the working gas, as well as for measuring the parameters of the plasma jet itself. The plasma temperature and density were determined from the intensity ratio of the spectral lines and their Stark broadening, respectively. Helium was used as the working gas, because all characteristic features of a PF discharge are well manifested in it. Moreover, the spectral lines of helium are more broadened by the electric field than other chemical elements (except for hydrogen), which is convenient for spectroscopic measurements at low plasma densities. The mechanisms for helium line broadening have been studied in detail and are described in many publications, and the calculated broadening parameters have been collected in tables (see, e.g., [3]). Since the number of helium spectral lines is relatively small, they are easy to identify and the lines that are not overlapped under considerable broadening can be usually chosen among them. Using the intensity ratio between the lines of neutral helium (HeI lines) and those of hydrogen-like helium ions (HeII lines), one can determine the plasma temperature. Helium can also be used as a diagnostic admixture to other working gases.

2. ARRANGEMENT OF THE EXPERIMENT AND SPECTRAL DIAGNOSTIC COMPLEX

The experiments on the generation of plasma jets were carried out at the PF-3 facility—a Filippov-type PF device with plane electrodes [4]. To study the dynamics of the plasma flow and the background plasma, a drift chamber (Fig. 1) [5, 6] consisting of three 300-mm-high 210-mm-diameter sections was

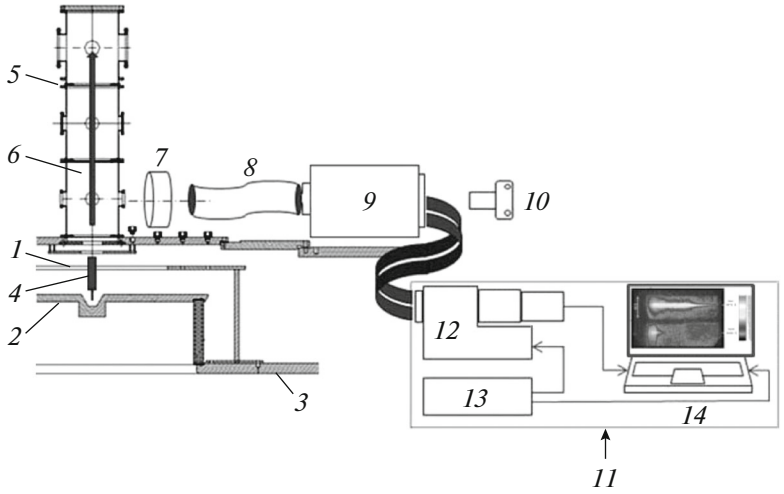

Fig. 1. Scheme of spectrum recording at the PF-3 facility: (*1*) cathode, (*2*) anode, (*3*) working chamber, (*4*) PF, (*5*) drift chamber, (*6*) plasma jet, (*7*) lens, (*8*) light guide, (*9*) STE-1 spectrograph, (*10*) photo camera adapter, (*11*) shielded box, (*12*) K008 image tube, (*13*) UPS, and (*14*) PC.

attached to the upper flange of the main discharge chamber of the PF-3 facility at a sufficiently large distance from the anode. The drift chamber has a set of diagnostic ports arranged equidistantly along the perimeter in the middle of each section at distances of 35, 65, and 95 cm from the anode plane. The working gas (helium) at a pressure of 3 Torr, which corresponds to the neutral helium atom density of 10^{17} cm^{-3}, fills both the discharge and drift chambers of the facility. The experiments described here were carried out in the first section of the drift chamber at a distance of 35 cm from the anode.

The PF-3 facility operates as follows. First, after the actuation of the facility spark-gap, a high voltage arises between the annular anode and the cathode. The voltage causes breakdown of the working gas over the surface of the glassceramic insulator. The formed current-carrying plasma is compressed by the Ampère force toward the vertical symmetry axis of the discharge, where plasma pinching occurs. As a result, a plasma pinch with a length of ~5 cm, temperature of $T \approx 0.5$ keV, and density of $N \approx 10^{19}$ cm^{-3} forms near the anode [4]. Its formation is accompanied by the generation an X-ray pulse with photon energies of >1 keV and a plasma jet propagating along the facility axis.

Our previous studies of the plasma jet dynamics [6] have demonstrated that the jet is highly inhomogeneous and its individual bunches with typical dimensions of ~1 cm move with different velocities. This imposes specific requirements on characteristics of the spectroscopic apparatus. In particular, the spectral lines that are used for diagnostics should be emitted from a plasma volume that should be large enough to provide the line intensity sufficient for measurements, but, on the other hand, should be smaller than the bunch size. Moreover, due to the expected broad range of the plasma densities, it is necessary to satisfy two contradictory requirements: on the one hand, the diagnostics should provide the necessary spectral resolution and, on the other hand, the spectral range under study should be sufficiently wide. The latter requirement excludes the application of such devices as the Fabry–Perot etalon. Under our experimental conditions, an STE-1 crossed dispersion spectrograph turned out to be optimal. This instrument allows one to record a panoramic spectrum of radiation in the range of 4500–9000 Å in three different orders with a linear dispersion of better than 0.1 mm/Å.

To simultaneously record the time behavior of the intensities and shapes of spectral lines, it is necessary to use a multichannel system—an image tube operating in the streak mode. We used a K008 image tube [7] which, together with the controlling PC and a UPS unit, was placed in a box shielded from electromagnetic interferences. Since the amplification coefficient of the image tube was insufficient to record a streak image under our experimental conditions, the tube was equipped with an additional intensity amplifier based on an EP-10 electron-optical image intensifier. The image was recorded from the screen of the image tube with a standard video camera and processed by means of the special-purpose KLEN 5M software [7], which automatically corrected the distortion and nonuniformity of the streak image and subtracted regular noises.

Figure 1 shows the scheme where the plasma jet propagates from the PF upward in the direction of the arrow. The image of the axial region of the jet was formed by a lens on the entrance end of the fiber light guide the exit end of which was attached to the entrance slit of the spectrograph. The fibers of the

light guide were arranged regularly, due to which the dimensions of both the entrance slit and the light guide determined those of the observation area, which was a rectangle with a 20-mm-long horizontal side and 1-mm-long vertical side. The images of two spectral intervals with the lines of interest to us were transferred by two light guides with regularly arranged fibers from the spectrograph output to the slit of the streak camera. The retuning of the diagnostic system to other spectral lines was performed by merely displacing the entrance ends of the light guides to the required part of the spectrum. A similar scheme of converging two spatially separated parts of the spectrum to one streak camera was previously applied by us in [8]. In addition, the entire time-integrated visible spectrum was recorded using a photo camera adapter. Thus, the diagnostic complex allowed us to record the panoramic spectrum of visible plasma radiation and study the time behavior of the intensities and shapes of at least two spectral lines in one experiment.

For the temporal analysis, two bright lines, $\lambda_1 = 5876$ Å and $\lambda_2 = 4686$ Å, were selected in the spectrum. The first line belongs to neutral helium, while the second one (P_α, the first line of the Paschen series), to hydrogen-like helium ions. The 2 × 6-mm ends of the light guides transferring the images of these lines to the entrance of the K008 image tube allow one to cover ~40-Å-wide spectral intervals in the vicinities of these lines, where there were no other appreciable spectral lines. The sensitivity of the spectrometric system in these two spectral intervals was relatively calibrated using an SIRSh 6-40 tungsten ribbon filament lamp and EOP-66 pyrometer. The ratio between the sensitivity of the spectrometric apparatus to the λ_2 line and that to the λ_1 line was found to be 2.7. The instrumental width of the spectrometric system, $\Delta_{ins}\lambda \approx 1.2$ Å, which is determined by the image tube and the light guides transferring the spectrum image, was measured in the course of the experiment (see Section 3).

In addition to the spectral diagnostics described above, the arrival of the plasma flow at the observation region (35 cm from the anode plane) was also detected by means of photoelectron multipliers (PEMs). The corresponding light signal was selected by collimators and fed to the PEMs through light guides. Collimation allows one to record optical radiation from a relatively small plasma volume along the chamber radius. The diameter of the conical region falling into the field of view of the collimator on the axis of the drift chamber did not exceed 5 mm. The PEMs recorded the instant of the plasma arrival at the observation region with a sufficiently high accuracy.

Among standard diagnostics of the PF-3 facility, we used an RPPD-11 semiconductor detector recording soft X-ray emission ($h\nu \geqslant 1$ keV) from the pinch region and a loop probe the signal of which was proportional to the time derivative of the discharge current of the facility. The peaks of these signals coincide well with the instant of the maximum pinch compression and can be conveniently used to synchronize the streak images of spectral lines with the discharge dynamics.

3. GENERAL FEATURES OF SPECTRUM DYNAMICS AND PLASMA PARAMETERS BEFORE THE ARRIVAL OF THE JET

In a long streak image of 60 μs per screen (Fig. 2), one can see that, at the instant of the arrival of the plasma jet at 8 μs, a light flare almost uniformly filling both the 40-Å spectral segments appears at a distance of 35 cm from the pinch. This flare lasts for 250 ns and is clearly recorded by the collimated PEMs (Fig. 3). For definiteness, it is the appearance of this signal that we consider the instant of the jet arrival. About 8 μs later, the profiles of the spectral lines become distinguishable against the continuous background. After the next 5 μs, the hydrogen-like ion line becomes invisible, while the neutral helium line, which gradually narrows and weakens, is seen during the entire sweep. Over 2–3 μs before the arrival of the plasma jet, a relatively weak (as compared to the jet) glow in the observed spectral intervals can be seen in the plot of the intensities (Fig. 2b). This time interval is marked in the streak image by two vertical lines. In faster streak images recorded with the maximum amplification, one can see other details in the time interval under consideration. Let us consider these details using shot no. 2014.10.23#5 as an example (Fig. 3).

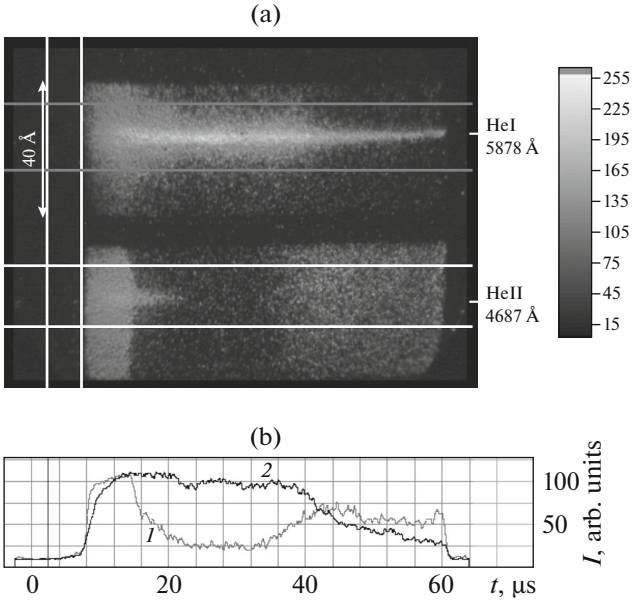

Fig. 2. (a) Streak image of the glow of two helium lines (on the right, the scale relating the darkening density to the glow intensity (in arb. units) is shown) and (b) intensities I of the (*1*) HeII and (*2*) HeI lines as functions of time (shot no. 2014.10.09#3).

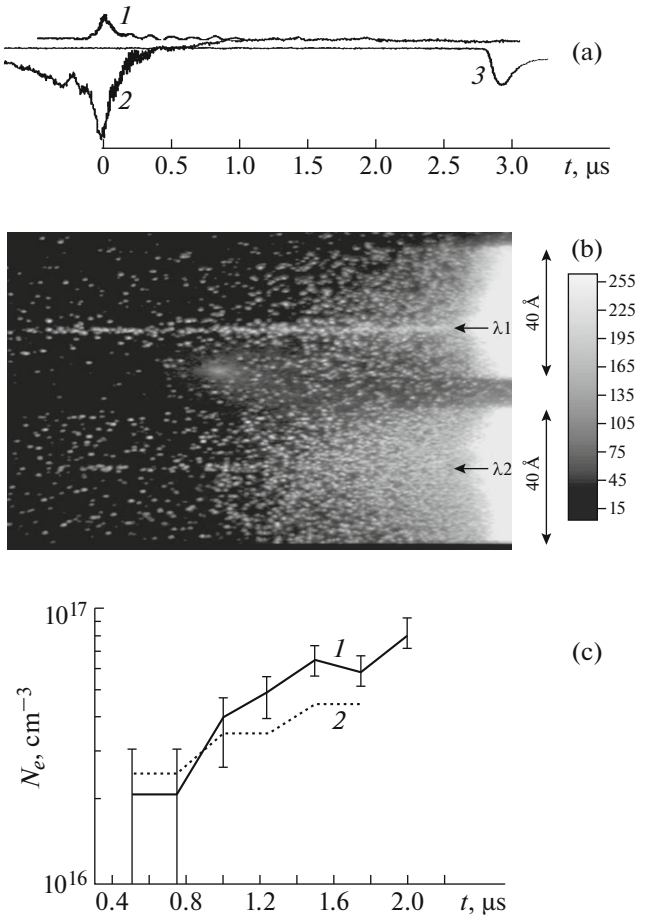

Fig. 3. Data from shot no. 2014.10.23#5: (a) synchronized waveforms (in arb. units) of the (*1*) X-ray intensity in the photon energy range of $h\nu \geqslant 1$ keV, (*2*) time derivative of the discharge current, and (*3*) light signal from the collimated PEM; (b) streak image of the glow of the neutral helium line ($\lambda_1 = 5876$ Å) and hydrogen-like helium ion line ($\lambda_2 = 4686$ Å) at a distance of 35 cm from the PF (on the right, the scale relating the darkening density to the glow intensity (in arb. units) is shown); and (c) time behavior of the plasma density N_e calculated from the Stark broadening of the lines (*1*) λ_1 and (*2*) λ_2 (here, the measurement errors related to the instrumental width and quantization step of the recording system are also shown).

Figure 3 presents the data of a typical experiment with a 3-μs-long sweep. Three curves in Fig. 3a show the time behavior of X-ray emission with photon energies of $\geqslant$1 keV (curve *1*), the time derivative of the total current (curve *2*), and the light recorded by the PEM through the collimator (curve *3*). Figure 3b presents a streak image of two ~40-Å-wide spectral segments, each of which contains the chosen spectral lines. Both spectral lines are seen almost from the very beginning of the sweep until the arrival of the jet at a time of 3 μs (Fig. 3b). Neutral helium, the line of which is marked by arrow λ_1, begins to glow somewhat earlier than X-ray emission with $h\nu \geqslant 1$ keV appears. The hydrogen-like helium line, the position of which is shown by arrow λ_2, appears only at the instant of the X-ray pulse and is seen not so clearly as λ_1. The excitation of neutral helium is probably caused by a softer X-ray emission that appears near the anode before the phase of maximum pinching and cannot be recorded by the detector [9]. The intensity and hardness of soft X-ray emission, which is strongly absorbed by the 35-cm gas column, seem to be insufficient to appreciably ionize helium. At this instant, it is convenient to measure the instrumental width of the spectrometric system ($\Delta_{ins}\lambda_1 \approx 1.2$ Å) by using the width of the line $\lambda_1 = 5876$ Å, because the glowing cold plasma is immobile and the Doppler broadening is negligible. The Stark broadening associated with the charged particle density is also much smaller than the instrumental width, because the width of the line λ_1 at the instant of the X-ray pulse does not increase as compared to that at the instant of its appearance, while the ion density before the X-ray pulse is substantially lower in view of the absence of the hydrogen-like line. After a short X-ray pulse with $h\nu \geqslant 1$ keV, the intensity of both lines drops by a factor of 1.5–2 over ≈0.7 μs. This is explained by the natural relaxation of excited lines over their characteristic times. Then, the intensity of the hydrogen-like helium line $\lambda_2 = 4686$ Å increases by a factor of 2–3 as compared to that at the instant of its first appearance. The glow of the neutral helium line $\lambda_1 = 5876$ Å first decreases and, then, increases again synchronously with λ_2. This second increase in the line intensity is most probably caused by the approaching plasma jet and the action of its thermal radiation with $h\nu \geqslant 20$ eV on the immobile gas in the drift chamber. This radiation results in the excitation of neutral helium, its ionization, and excitation of hydrogen-like helium. In other words, the jet behaves as if it "invades" through the gas.

The second increase in the intensity of helium lines in the time interval t_1 from 1 to 2 μs after the maximum of the X-ray pulse can also be explained by the arrival of the first fast plasma bunches generated in the axial direction by the plasma pinch. The average velocity of the first plasma bunches at a distance of 35 cm is $V_{av1} = 35/t_1 = 3.5 \times 10^7$ cm/s, which corresponds to the energy of the translational motion of ions along the axis, $E_{He} \approx 2.5$ keV. With allowance for significant energy expenditures on the motion of fast bunches in the immobile gas, their initial energy must be appreciably higher. To clarify this issue, it is necessary to carry out special experiments.

The plasma temperature can be estimated from the observed intensity ratio (see Fig. 4) of the spectral lines [10]. This ratio is the result of averaging carried out within the local thermodynamic equilibrium model when it is still applicable at an electron density of $N_e \approx 10^{18}$ cm^{-3}, as well as within the coronal model at densities of $>10^{16}$ cm^{-3} and temperatures of $T_e >$ 3.5 eV. In this temperature range, the populations of

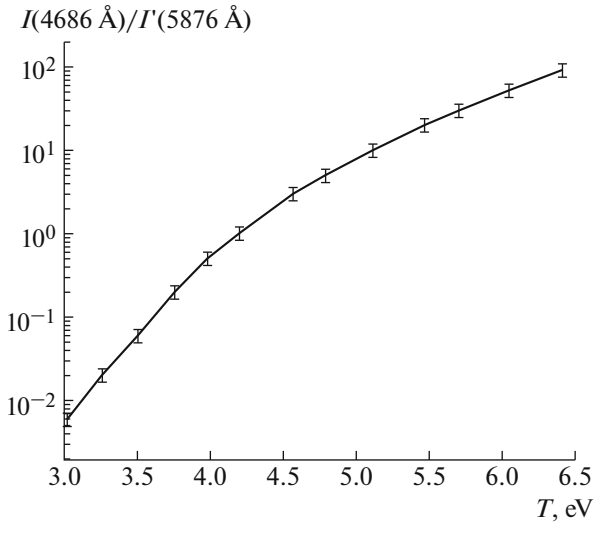

Fig. 4. Intensity ratio of the HeII 4686 Å (I) and HeI 5876 Å (I') lines as a function of the plasma temperature.

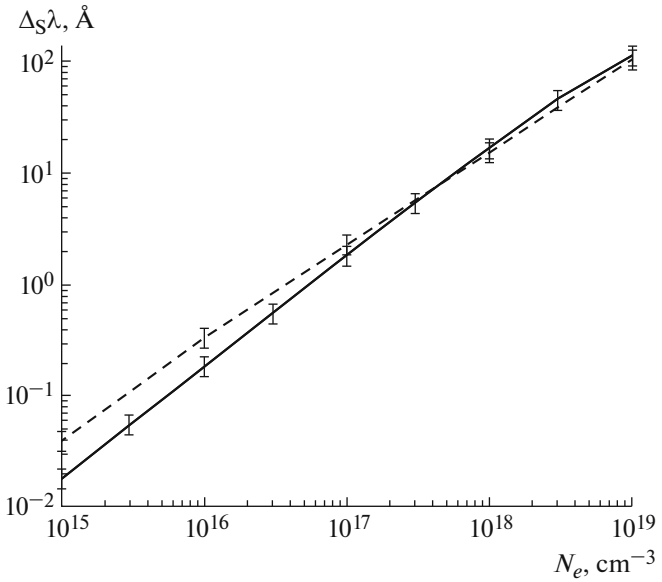

Fig. 5. Stark FWHMs $\Delta_S\lambda$ of the HeI 5876 Å line (solid curve) and HeII 4686 Å line (dashed curve) as functions of the plasma density at $T = 4$ eV.

the upper states of the transitions under consideration are in the coronal equilibrium with ions in higher ionization states, namely, for the transition $\lambda_1 = 5876$ Å HeI with singly ionized helium and the transition $\lambda_2 = 4686$ Å HeII with bare helium nuclei. In the temperature and density ranges of $3.5 < T_e < 6$ eV and $10^{16} < N_e < 10^{18}$ cm^{-3}, the error in determining the temperature in Fig. 4 is less than 20%. In this and other calculated dependences presented in our paper, the errors are shown graphically. In the time interval from 1 to 2 μs after the maximum of the X-ray pulse, the intensity ratio of the HeII P_α 4686 Å and HeI 5876 Å lines ranges from 1 to 2, which corresponds to the plasma ionization temperature of 4.3 eV. For the intensity ratio of 0.01 and less, which in our experiments corresponds to the disappearance of the hydrogen-like ion line on the image tube screen, the temperature T_e does not exceed 3 eV. We recall that by the ionization temperature we mean the electron temperature that yields the observed ratio of the ion densities for two different ionization states under the conditions corresponding to the used plasma model.

If the width of the line $\lambda_1 = 5876$ Å is calculated 1 μs after its appearance by subtracting the instrumental width from the measured line width $\Delta_{exp}\lambda \approx 1.32$ Å according to the quadratic formula $\Delta_S\lambda_1 \approx (\Delta^2_{exp}\lambda - \Delta^2_{ins}\lambda)^{1/2} = 0.54$ Å and the obtained broadening is assumed to be exclusively the Stark broadening caused by the quasi-static Holtsmark ion field and electron impacts, then, according to calculations [10], the estimated plasma density (Fig. 5) is $N_i \approx 2 \times 10^{16}$ cm^{-3}, i.e., the degree of ionization in terms of the initial gas density is 0.2.

As the jet approaches the observation region, the lines λ_1 and λ_2 broaden and one can trace the dynamics of the increase in the ion density. The time dependence of the plasma density in shot no. 2014.10.23#5, synchronized with the streak image of the spectral lines, is presented in Fig. 3c. As is seen from Fig. 3b, the width of the line λ_2 of hydrogen-like helium rapidly increases as the jet approaches the observation region. The line profile begins to be distorted 1.2 μs after the X-ray pulse and, by the second microsecond, becomes strongly irregular, which impedes correct estimation of the line width. The profile of the λ_1 line is distorted weaker than that of the line λ_2, and its width can be successfully determined for a longer time. Note that an increase in the line width can be caused not only by the adiabatic electric field of ions and electron impacts, but also by strong turbulent plasma noise. In view of the afore said, the estimate of the plasma density obtained from the width of a line with a distorted profile should be treated only as an upper estimate. This especially concerns the plot in Fig. 3 after the second microsecond.

When interpreting the spectra, it is of fundamental importance to take into account the line self-absorption determined by the plasma optical thickness τ. In the process of self-absorption, the line broadens by factors of $\sqrt{\ln(\tau)}$, $\sqrt{\tau}$, and $\tau^{2/5}$ for the Doppler profile γ_D, Lorentz profile γ, and Holtsmark profile $\Delta\omega_H$, respectively [11]. Radiation absorption in the peripheral plasma can lead to a dip in the middle of the line profile. According to calculations carried out in terms of the equilibrium collisional-radiative plasma model [12], the optical thickness of helium plasma at $T_e = 4$–6 eV, $N_{He} = 4 \times 10^{16}$ cm^{-3}, and plasma layer thickness

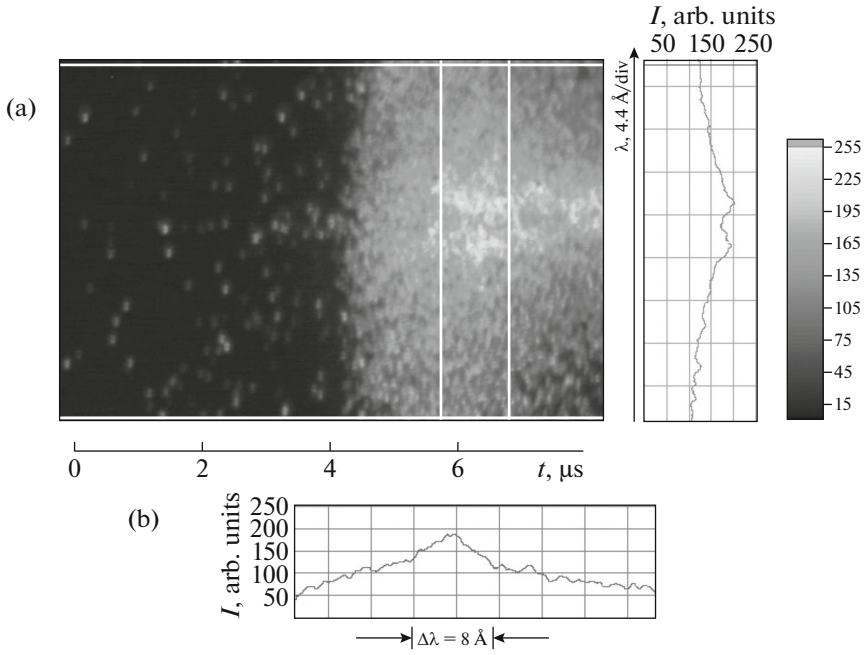

Fig. 6. (a) Streak image of the line $\lambda_1 = 5876$ Å and time-averaged profile of the line emitted from the dense jet core (on the right, the scale relating the darkening density to the glow intensity (in arb. units) is shown) and (b) profile of the spectral line $\lambda_2 = 4686$ Å and its FWHM averaged over the same time interval (shot no. 2014.10.09#4). The 1-μs-long averaging time interval is shown by the straight vertical lines in the streak image.

of 10 cm is $\tau_2 = 1.04$ for $\lambda_2 = 4686$ Å, which leads to an additional increase in the Holtsmark line width only by 2%. For the line $\lambda_1 = 5876$ Å in plasma with a density of 2×10^{17} cm^{-3}, the optical thickness turns out to be one order of magnitude lower. This means that during 2.5 μs after the maximum of the X-ray pulse, up to $N_e \approx 2 \times 10^{17}$ cm^{-3}, self-absorption of the line λ_1 in the considered temperature range can be neglected when estimating the density before the jet arrival.

4. JET PARAMETERS

At the instant of the arrival of the plasma jet at the observation region (this is the ninth microsecond of the sweep in Fig. 2 and the fifth microsecond in Fig. 6), instead of lines, one can see an almost uniform glow in the entire spectral interval of 40 Å surveyed by the light guide aperture. This glow can be attributed to the action of the shock wave on the working gas. The shock wave formed upon the supersonic propagation of the jet through the gas is able to significantly ionize the gas, and the observed glow can be caused by the continuous bremsstrahlung of free electrons on helium nuclei. In this case, the plasma temperature can be estimated from below from the absence of hydrogen-like ion lines in the plasma radiation spectrum. Assuming that this takes place at least at 95% ionization of hydrogen-like helium, we find that the plasma temperature estimated by using the results of computations [12] performed according to the collisional-radiative model is $T \geqslant 8$ eV (Fig. 7).

After 6 μs, spectral lines appear in Fig. 6, and one can estimate their widths and intensities. To the right

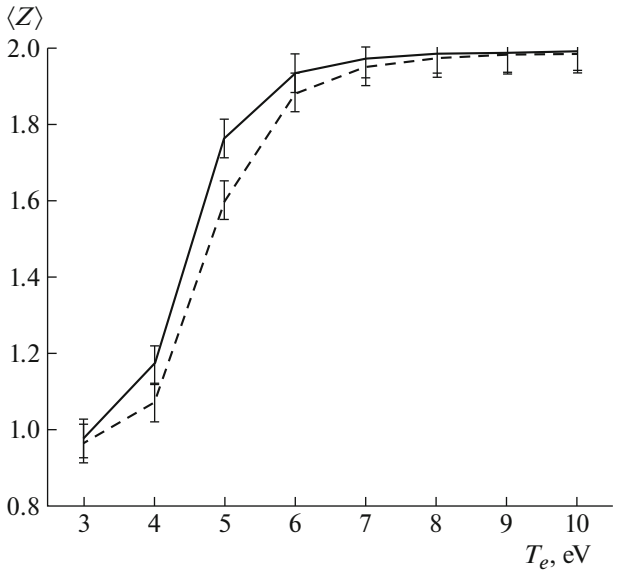

Fig. 7. Average ion charge calculated by the collisional-radiative model as a function of the helium temperature for two electron densities: $N_e = 10^{17}$ cm^{-3} (solid line) and $N_e = 3 \times 10^{17}$ cm^{-3} (dashed line).

in Fig. 6a, the profile of the line λ_1 is shown in combination with the streak image leftward. In Fig. 6b, one can see the profile of the line λ_2 at the time instant under consideration. For the jet in this and other PF-3 shots, the intensity ratio $I(\lambda_2)/I(\lambda_1)$ of the considered lines ranges from 3 to 11, which, according to the plot in Fig. 4, corresponds to a plasma temperature of $T \approx$ 5 eV. The average propagation velocity of the plasma bunch at a distance of 35 cm, from the maximum of the X-ray pulse to the maximum intensity of the observed lines, was found to be $V_{av2} = 10^7$ cm/s.

Let us estimate the plasma density. When the intensity of lines in the jet is at maximum, a dip (typical of line self-absorption) usually appears in the middle of the profile of the line $\lambda_1 = 5876$ Å, e.g., during 1 μs in shot no. 2014.10.09#4 (Fig. 6). Accordingly, the full width at half-maximum (FWHM) of the line, $\Delta_S\lambda_1 \approx 10$ Å, is also overestimated due to the dip in the central part of the line profile. The background illumination of the image tube screen was taken to be 50 (see Fig. 6b). Note that the intensely radiating jet efficiently excites the ambient neutral helium in diagnostic ports, which results in the additional self-absorption of the line λ_1. In connection with this, it is better to estimate the density from the FWHM of the hydrogen-like helium line P_α, $\Delta_S\lambda_2 = 4$ Å, according to the dependence shown in Fig. 5, because its self-absorption at this time is significantly less (Fig. 6b) than that of the observed neutral helium line. Thus, the maximum plasma density in the jet can be estimated from above as $N_e \sim 2 \times 10^{17}$ cm^{-3}, which exceeds the initial helium density in the working chamber. We note again that the line broadening can be also caused by low-frequency turbulent electric fields.

5. HIGH-FREQUENCY PLASMA OSCILLATIONS

Before and after the arrival of the hot jet, dips and peaks in the profiles of the lines $\lambda_1 = 5876$ Å and $\lambda_2 = 4686$ Å are clearly seen on short time intervals (Fig. 8). They may form under the joint action of low- and high-frequency (HF) electric microfields [13–15]. The dips and peaks in the line wings indicate the presence of Langmuir oscillations, which become especially pronounced when their frequency ω_{pe} coincides with the frequency shift $\Delta\omega$ of spin-orbital components of the line in an adiabatic electric field. In the presence of Langmuir oscillations, the peaks are typically arranged symmetrically relative to the central component of the line with a shift by ω_{pe}, as is observed in our experiments. The frequency of Langmuir oscillations is determined by the electron density, $\omega_{pe}\,[\mathrm{s}^{-1}] = (4\pi N_e e^2/m_e)^{1/2} = 5.64 \times 10^4 (N_e\,[\mathrm{cm}^{-3}])^{1/2}$, where e and m_e are the charge and mass of an electron, respectively. To associate the measured shift of the peak $\Delta\lambda_p$ from the line center (see Fig. 8) with the electron density, it is convenient to use the following formula, which is derived from the previous expression: $N_e\,[\mathrm{cm}^{-3}] = 1.1\times10^{29}(\Delta\lambda_p)^2/\lambda_0^4$, where λ is in Å.

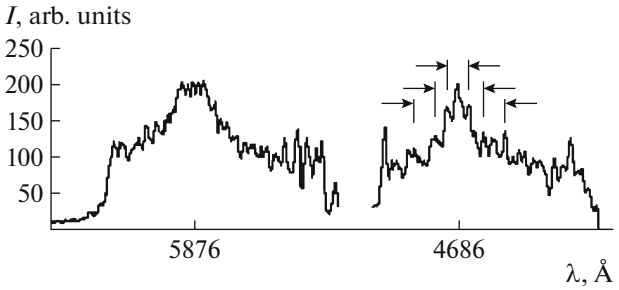

Fig. 8. Profiles of the 5876 and 4686 Å helium lines in the plasma jet (shot no. 2014.10.09#5), recorded at 5 μs after the jet arrival. The arrows demonstrate the symmetric positions of the peaks with respect to the center of the HeII 4686 Å line. The widths of both two spectral intervals are 40 Å.

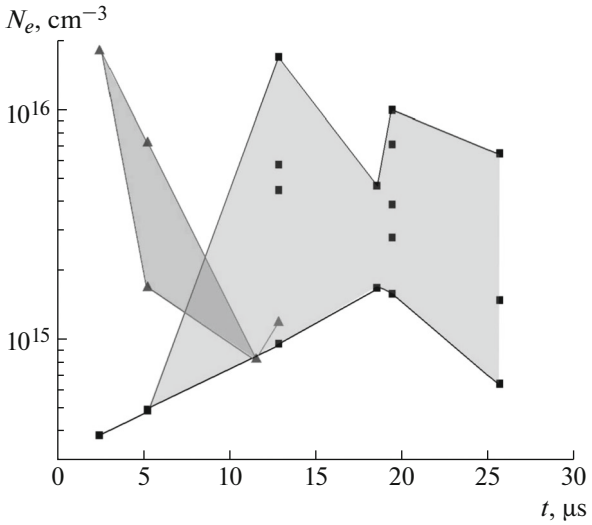

Fig. 9. Time behavior of the plasma density recovered from the Langmuir peaks in the profiles of the HeII 4686 Å line (▲) and HeI 5876 Å line (■) (shot no. 2014.10.07#5). The solid lines join the instantaneous extreme values of the density recovered from the same spectral line (the density intervals are shaded with gray). The measurement errors are 20 and 80% at densities of 10^{16} and 4×10^{14} cm^{-3}, respectively. The beginning of the plot corresponds to the instant of the jet arrival.

Figure 9 shows the typical time behavior of the plasma density recovered from the arrangement of peaks in the line profile (shot no. 2014.10.07#5). Here, the time is counted from the maximum of the glow of the jet core. It follows from Fig. 9 that the dense plasma formed in the pinch and propagating in the drift chamber is inhomogeneous. The presence of a series of frequencies ω_{pe} existing at each time instant indicates that the plasma bunch is structured and con-

sists of plasma layers with different densities. The values of the plasma density recovered from the peaks of the HeII 4686-Å line lie in the range of $N_e = 8 \times 10^{14}$–2×10^{16} cm^{-3}, while those recovered from the peaks of the HeI 5876-Å line lie in the range of $N_e = 4 \times 10^{14}$–10^{16} cm^{-3}. These results can be explained by the superposition of radiation from plasma bunches with a nonuniform density. The peaks corresponding to even higher densities can lie on the line wings too far from the line center and cannot be detected because of the noise of the recording system. Earlier, we observed the inhomogeneity of the plasma jet on streak images in experiments with different gases [6].

To understand the nature of the observed Langmuir oscillations, let us estimate the electric field strength by means of the technique based on the measured deviation of the dip from the line center $\Delta\lambda_d$ and its half-width $\Delta\lambda_{1/2}^d$, defined as the distance to the neighboring peak. For typical experimental values obtained for the HeII 4686 Å line, namely, $\Delta\lambda_d = 7.7$ Å and $\Delta\lambda_{1/2}^d \approx 1.2$ Å at $N_e = 10^{16}$ cm^{-3}, the formula $\Delta\lambda_{1/2}^d = (7\times10^9 E_{HF}/\omega_{pe})\Delta\lambda_d$ from [14] yields the following amplitude of the HF electric field: $E_{HF} \approx$ 50 kV/cm. This formula is applicable in the case of strong HF fields exceeding the Holtsmark field, $E_{HF} > 2.6|e|N^{2/3} \approx 17$ kV/cm. In our experiments, this condition is satisfied. Because of the relatively large instrumental width, it seems impossible to measure the amplitude of the HF electric field at lower densities.

In plasma in which the number of particles N_D in the Debye sphere is small, HF electric fields with such strengths may arise due to thermal fluctuations of the charged particle density, i.e., they may be, in a sense, "equilibrium" ones. The energy density of such thermal noise can be estimated from the relationship $(E_0^2/4\pi)/N_eT \approx 1/N_D$ (in CGSE units) [14]. Here, $N_D = N_e r_D^3 = 4\times10^8\sqrt{T^3/N_e}$, where the temperature and density are in eV and cm^{-3}, respectively. For a plasma jet with a temperature of 5 eV and density of 10^{16} cm^{-3}, the number of particles in the Debye sphere is $N_D \approx 50$ and the amplitude of the equilibrium noise field is $E_0 \approx 50$ kV/cm.

Comparison of E_{HF} with the obtained value of E_0 indicates that, for the density range under consideration, the observed noise may well be of equilibrium nature.

By the end of the sweep (Fig. 2), plasma noises gradually decrease and the HeI 5876 Å line gradually narrows, i.e., the plasma density is reduced. After 15 μs, the hydrogen-like ion line disappears, which indicates a decrease in the temperature below 3 eV.

6. CONCLUSIONS

A diagnostic complex has been created at the PF-3 facility. The complex allows one to recover the time behavior of the parameters of the plasma jet and ionized immobile gas at a distance of 35 cm from the PF from the time dependences of the intensities and shapes of spectral lines of neutral helium and hydrogen-like helium ions.

The measurements have shown that the immobile gas is first ionized by the X-ray pulse of the pinch. Estimates show that the ionization temperature is about 4 eV and the degree of ionization does not exceed 0.2. About 1 μs later, the increase in the glow intensity is most probably caused by the approaching plasma jet and the action of its intrinsic radiation with $h\nu \geqslant 20$ eV on the immobile gas. The plasma density estimated from the Stark broadening of lines at this time is $N_i \approx 2 \times 10^{16}$ cm^{-3}. During the next 2.5 μs, the ion plasma density gradually increases to $\approx 2 \times 10^{17}$ cm^{-3}, while the temperature somewhat grows.

The jet has a high brightness as compared to the immobile plasma and moves with a velocity of 10^7 cm/s along the system axis. At the instant of the jet arrival at the observation region, the spectral lines under study are indistinguishable against the background continuous radiation and the temperature can exceed 8 eV. After 1–2 μs, the lines are seen again, which makes it possible to estimate from above the density of the jet from the Stark broadening of lines with allowance of its self-absorption. The ion density in this stage is $N_i \approx 2 \times 10^{17}$ cm^{-3} and the plasma temperature is $T \approx 5$ eV.

Just before the arrival of the jet, as well as in the tail of the jet, high-frequency plasma noises are observed in the immobile plasma. The plasma jet formed in the pinch and propagating in the drift chamber is strongly inhomogeneous in both the radial and longitudinal directions. The plasma bunch densities, which are estimated from below exclusively from the frequencies of Langmuir oscillations, lie within the range of $N_i \approx 4 \times 10^{14}$–$10^{16}$ cm^{-3}. The electric fields of Langmuir oscillations are at a level of 5–50 kV/cm, which does not contradict their equilibrium nature.

The observed different mechanisms of spectral line broadening, such as HF noise and the large optical plasma thickness in spectral lines, demonstrate that it is necessary to improve the spectroscopic technique in order to investigate the parameters of the plasma jets in more detail. We plan to do this in our subsequent study.

ACKNOWLEDGMENTS

We are grateful to K.V. Chukbar for fruitful discussions. This work was supported in part by the Russian Foundation for Basic Research (project nos. 14-02-00179a, 14-02-31473-m, 14-29-06085 ofi_m, and

14-02-90427 Ukr_a) and the National Academy of Sciences of Ukraine (project no. 17-02-14).

REFERENCES

1. *Astrophysical Jets and Their Engines (NATO ASI Series, Ser. C: Math. Phys. Sci., Vol. 208),* Ed. by W. Kundt (Reidel, Dordrecht, 1986).
2. V. G. Surdin, *Birth of Stars* (Editorial URSS, Moscow, 2001) [in Russian].
3. H. R. Griem, *Spectral Line Broadening by Plasmas* (Academic, New York, 1974).
4. *Encyclopedia of Low-Temperature Plasma,* Ed. by V. E. Fortov, Ser. B, Vol. IX-2: *High-Energy Plasmadynamics,* Ed. by A. S. Kingsep (Yanus-K, Moscow, 2007) [in Russian].
5. V. Krauz, V. Myalton, V. Vinogradov, E. Velikhov, S. Ananyev, Yu. Vinogradova, S. Dan'ko, Yu. Kalinin, G. Kanaev, K. Mitrofanov, A. Mokeev, A. Nashilevsky, V. Nikulin, A. Pastukhov, G. Remnev, et al., Phys. Scr. **161**, 014036 (2014).
6. S. S. Anan'ev, S. A. Dan'ko, V. V. Myalton, Yu. G. Kalinin, V. I. Krauz, V. P. Vinogradov, and Yu. V. Vinogradova, Vopr. At. Nauki Tekh., Ser. Termoyad. Sintez **36** (4), 102 (2013).
7. www.bifocompany.com
8. S. S. Anan'ev, S. A. Dan'ko, and Yu. G. Kalinin, Vopr. At. Nauki Tekh., Ser. Termoyad. Sintez **32** (2), 43 (2009).
9. S. A. Dan'ko, K. N. Mitrofanov, V. I. Krauz, V. V. Myalton, A. I. Zhuzhunashvili, V. P. Vinogradov, A. M. Kharrasov, S. S. Anan'ev, Yu. V. Vinogradova, and Yu. G. Kalinin, Plasma Phys. Rep. **41**, 882 (2015).
10. H. Griem, *Plasma Spectroscopy* (McGraw-Hill, New York, 1964).
11. V. I. Derzhiev, A. G. Zhidkov, and S. I. Yakovlenko, *Ion Radiation in Dense Nonequlibrium Plasma* (Energoatomizdat, Moscow, 1986) [in Russian].
12. http://nlte.nist.gov/FLY/
13. H. R. Griem, A. C. Kolb, and K. Y. Shen, Phys. Rev. **116**, 4 (1959).
14. E. A. Oks and V. A. Rantsev-Kartinov, Sov. Phys. JETP **52**, 50 (1980).
15. G. V. Sholin, Sov. Phys. Doklady **15**, 1040 (1970).

Translated by A. Nikol'skii